Theoretical Notes TN 220
Note 220

DNA 3094F

RESEARCH ON INTERNAL ELECTROMAGNETIC PULSE PHENOMENA

Daniel C. Osborn
Andrew R. Wilson
Systems, Science and Software, Inc.
P. O. Box 1620
La Jolla, California 92037

2 October 1973

Final Report

CONTRACT No. DNA 001-72-C-0088

THIS WORK SPONSORED BY THE DEFENSE NUCLEAR AGENCY
UNDER NWED SUBTASK EB089-05.

Prepared for
Director
DEFENSE NUCLEAR AGENCY
Washington, D. C. 20305

PREFACE

This report was prepared in the Technology Department, Systems and Software Division of Systems, Science and Software. The participants in the study and their areas of contribution are identified below:

D. C. Osborn	Project management, test definition and direction, data analysis
A. R. Wilson	Theoretical analysis of data
B. S. Flanagan	Test instrumentation, sensor fabrication and test, and vacuum system fabrication
G. Ehlers	Tank fabrication liaison, test support
D. A. Meskan	Management of second HERMES test
E. A. Day	Tank design
G. Benford	Theoretical support
R. Bryson	Data reduction
K. Pyatt D. Grine G. Seay A. Petschek	Program review and guidance

The project also acknowledges the support of the personnel at the Sandia HERMES facility, especially R. Schuch, J. Harness and L. Posey and the instrumentation support of the Bendix personnel at the Nevada Test Site. The assistance of A. Bromborsky, Harry Diamond Laboratory, in running the DELIT code and of B. Brennan, Stanford Research Institute, in digitizing the oscilloscope waveforms is also gratefully acknowledged. Finally, the efforts of M. A. Turner and D. Baumgarten in preparing the final draft are especially appreciated.

TABLE OF CONTENTS

TABLE OF CONTENTS (continued)

LIST OF ILLUSTRATIONS

LIST OF ILLUSTRATIONS (continued)

LIST OF ILLUSTRATIONS (continued)

LIST OF ILLUSTRATIONS (continued)

LIST OF TABLES

1. INTRODUCTION AND SUMMARY

1.1 OBJECTIVES

The primary objective of this study was the measurement of IEMP fields and IEMP-induced cable currents, as functions of gas pressure, in a large vacuum tank. The tank geometry was selected to minimize problems of predicting IEMP fields. Exposures took place at the HERMES facility. Measurements included electric and magnetic field maps, current induced on cables in the tank and the variations of these quantities with tank pressure. A second objective was the interpretation of the experimental results in view of available theoretical predictions of IEMP effects.

1.2 BACKGROUND

Experimental measurements of IEMP fields and cable signals were conducted previously in a large vacuum test chamber at HERMES and at an underground nuclear test.[1] The test chamber used was a one meter diameter cylinder, approximately one meter long, with dished end-faces and a large manhole in the side for access into the tank. Radiation impinged on the cylindrical surface perpendicular to the tank axis in these tests.

In order to simplify the prediction of the IEMP fields, a more idealized tank geometry was proposed for further flash x-ray studied. A flat-faced cylindrical tank was suggested, where the cylinder axis would coincide with the axis of the radiation source. The primary emitting surface would be flat

in this case, producing fields that would be axially symmetric. The electric and magnetic field sensors, tank hardware and vacuum system used on the previous program could be usefully applied to this study.

1.3 PROGRAM SUMMARY

This report presents the results of the six-month experimental study of the IEMP fields and cable signals in a one meter long, one meter diameter cylindrical vacuum tank. The exposures were conducted at the HERMES facility. The project designed and fabricated the cylindrical test chamber, discussed in Section 2, incorporating such features into the design as hinged front and rear doors and removable wall current monitors. The signal outputs for several types of magnetic and electric field sensors and current probes were modified to obtain differential outputs and to improve impedance matching, and are described in Section 3. All electric and magnetic sensors used were calibrated in a fast rise electromagnetic field produced in the large coaxial tester designed on the previous project. In addition, various tests were conducted with the sensors themselves on several shots to verify their performance in the radiation environment.

Magnetic and electric field measurements presented in Section 4 were made in various locations in the tank, for a pressure range from 0.35 microns to atmospheric pressure. Good agreement was obtained between the outputs of magnetic loops at the walls and the interior of the tank and the fields that were calculated from dosimetry data using the results of the DELIT electron emission code computed for the project by the Harry Diamond Laboratory. Also, the observed variation in electric field at the walls with air pressure was seen to

be in agreement with the variation predicted by a space charge model described in Section 5.3. Current density measurements made using a Rogowski coil on the tank axis were quite close to the values calculated from the magnetic loop measurements.

Several electric and magnetic field measurements were also made with the tank very close to the radiation source, so that three times the normal dose rates were obtained. The field measurements at these dose rates are consistent with the predictions, also. (See Sections 4.3 and 4.8, and Section 5.)

The signals induced on coaxial cables were measured at various locations and pressures in the tank, and are described in Section 4.12. These signals, in contrast to the above, were much more complex and not so easily interpreted.

Both the electric and magnetic field measurements exhibited a consistent secondary structure made up of damped oscillations at various frequencies, and discussed in Sections 4.6, 4.10 and 5.4. A high frequency oscillation, very likely associated with the cavity resonances, is observed on the magnetic loop signals. The oscillations decrease in amplitude with increasing air pressure. In addition, oscillations observed on the electric field sensors are seen to increase in frequency with increasing air densities. Both relationships may be useful as diagnostic tools, for an independent measurement of secondary electron densities.

As a result of this study, it appears that the sensors employed here can be relied upon to give good measurements of IEMP effects in more complex geometries.

2. EXPERIMENTAL EQUIPMENT AND INSTRUMENTATION

2.1 TEST CHAMBER

The test chamber designed and used for IEMP testing at the HERMES facility is shown in Figure 2.1. The chamber is an aluminum vacuum-tight cylinder, one meter long and one meter in diameter, with flat gasketed front and rear faces that are hinged to allow access into the tank. Both doors (faces) are 1.0 inch thick, while the cylinder wall is 0.25 inch thick. For mobility, the tank is bolted to a four-legged dolly fitted with casters, positioning the tank axis at 56.5 inches from the floor. A photograph of the tank is shown in Figure 2.2.

Each door hinge was designed to accommodate a current sensor assembly to measure current flow between the door and the cylinder wall. Each door is isolated from the cylinder flange with a 0.75 inch gasketed Plexiglas ring and an insulated hinge. A total of 144 beryllium copper contact fingers speced uniformly around the circumference provide the electrical connection between the wall and door. A miniature current probe surrounding one contact finger monitors the current. Both current monitor assemblies may be removed to verify that their presence does not perturb the internal fields. A photograph of the interior of the tank is shown in Figure 2.3.

Electrical connections to sensors inside the tank are made through any of 44 feedthrough ports in the faces and in the wall. A small gasketed Plexiglas collar electrically isolates each coaxial feedthrough connector from the tank. Series HN vacuum feedthrough (Gremar No. 13953) are used.

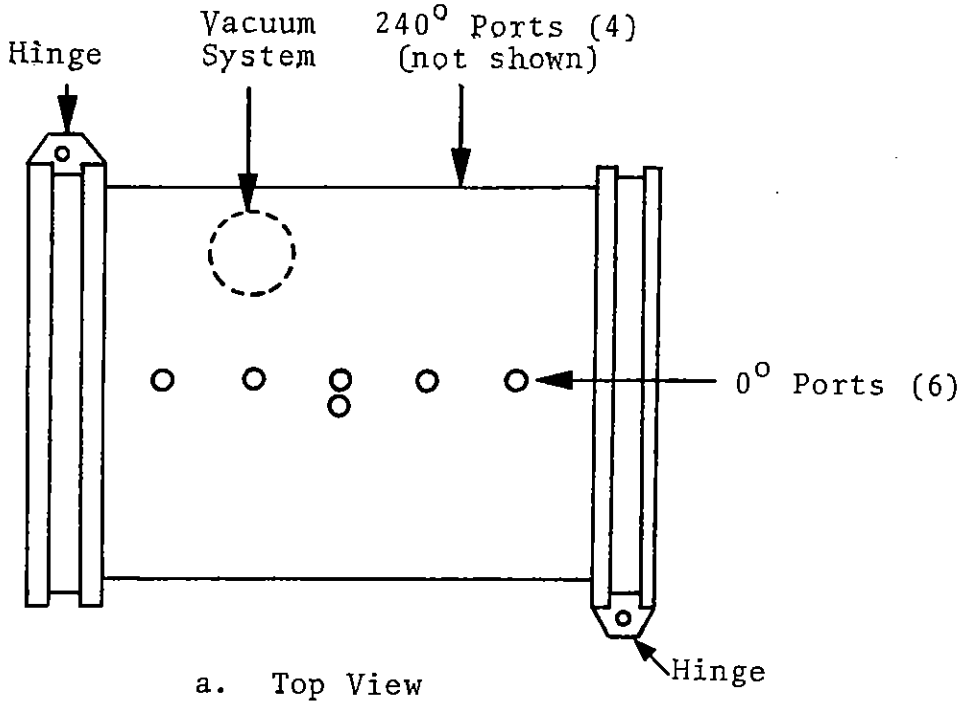

a. Top View

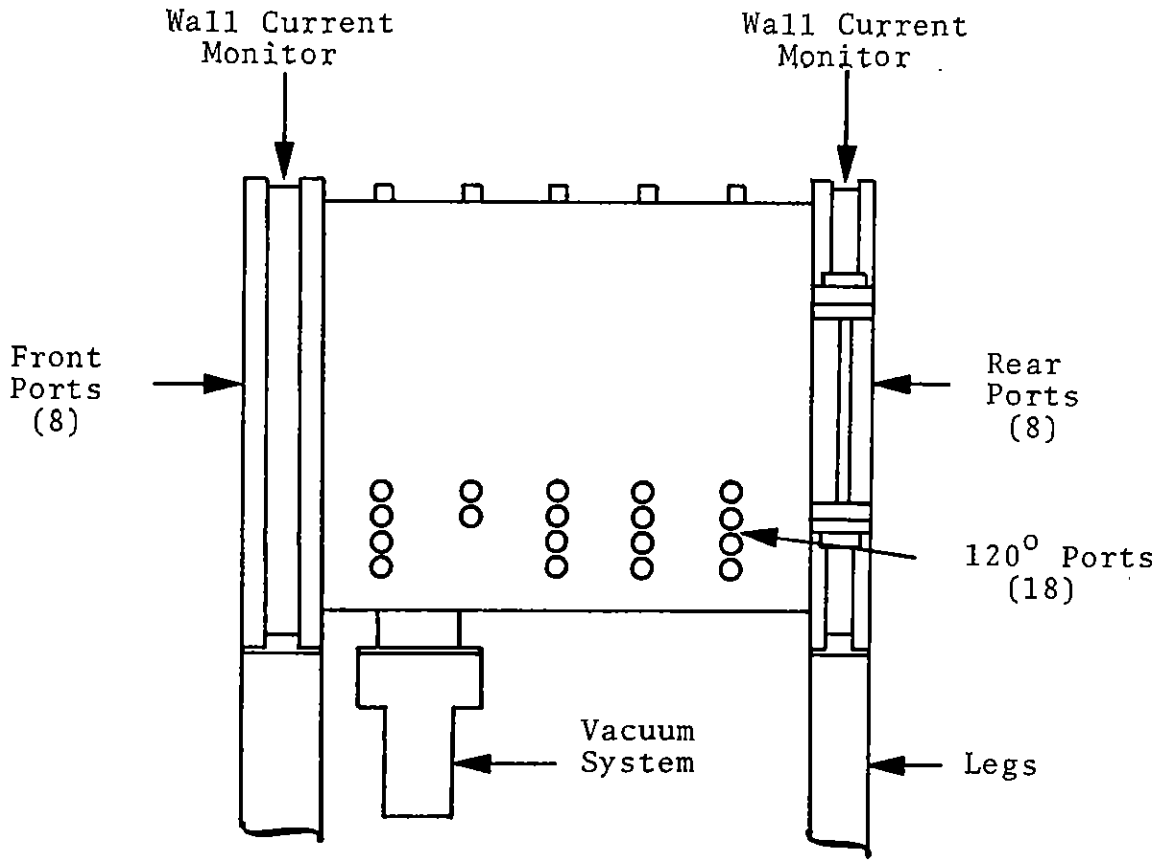

b. Side View

FIGURE 2.1

Test Chamber

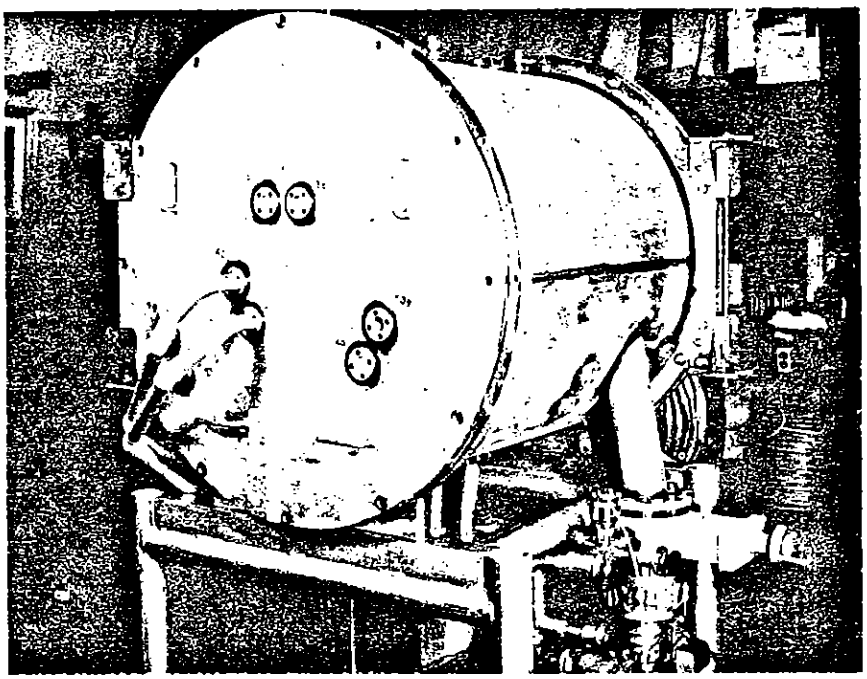

FIGURE 2.2
Photograph of Test Chamber, Rear

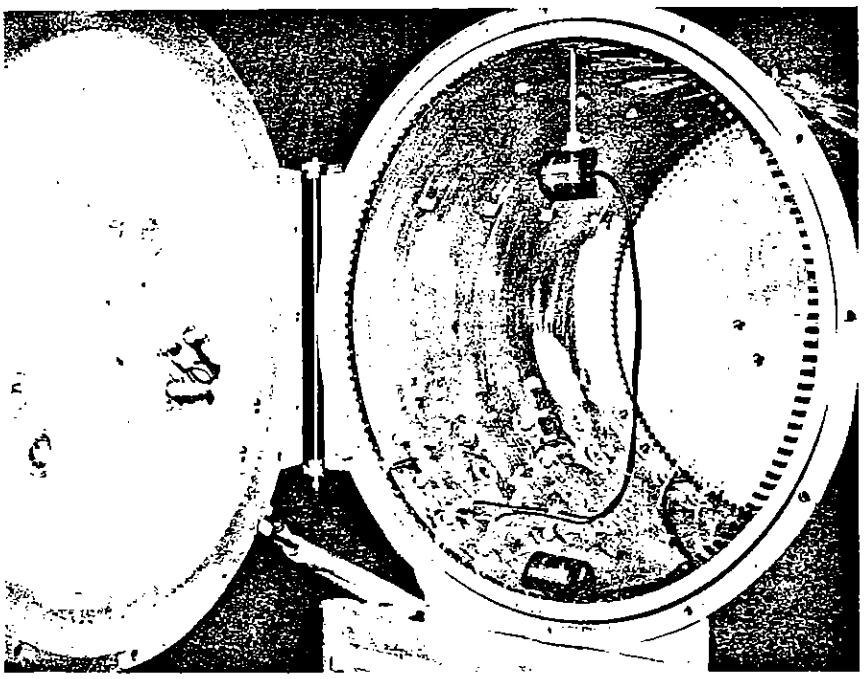

FIGURE 2.3
Photograph of Test Chamber Interior, from the Rear

Table 2.1 gives the distribution of the 44 ports. The cylinder wall ports are located in three groups, 120° apart. Each group is designated by the value of the coordinate vector θ in a right-hand cylindrical coordinate system, where $\theta = 0^{\circ}$ corresponds to the top of the tank (see Figure 2.1). The largest number of ports are positioned at the 120° azimuth. Most of the magnetic field and radial electric field measurements were made here to minimize patch cable length to the adjacent junction box.

TABLE 2.1
FEEDTHROUGH PORTS

Location	Quantity
Front Face	8
Wall, 0° Azimuth	6
Wall, 120° Azimuth	18
Wall, 240° Azimuth	4
Rear Face	8

Traverse rods, with vacuum fittings, were made to allow sensors to be repositioned in the tank without breaking vacuum. The rod fittings are compatible with the feedthrough ports and are used vertically in the 0° ports. A rod supporting a magnetic field sensor is shown in Figure 2.3. In this figure can be seen the small tapped blocks spot welded at various points in the tank and the tapped holes in the side ports used for sensor and cable mounting. Typical locations of the electric and magnetic field sensors are also shown here.

The vacuum system used here consists of a Veeco 4-inch water-cooled diffusion pump (Model EP4-1, with a water-cooled baffle), a Welch two-stage fore pump (Model 1397B), and appropriate valving. The diffusion pump and a 4-inch gate

valve are bolted to a flanged port below the tank. A Plexiglas spacer and insulating bolts electrically isolate the vacuum system from the tank. To minimize perturbations of the internal wall currents, the tank wall at the vacuum port was not removed, but was simply drilled with closely spaced three-quarter-inch holes.

2.2 EXPERIMENTAL CONFIGURATION

The experimental setup used at HERMES is shown in Figure 2.4. The tank and dolly stand on a 6 foot square wooden sled that also supports the junction (J) box. The sled has casters for mobility and raises the tank axis to coincide with the HERMES FXR radiation axis. The mechanical fore pump rests on the HERMES platform on shock mounts, rather than on the slid, to reduce vibration.

A radio frequency interference (RFI) shielding system is provided to reduce noise from both electromagnetic fields and electrons in the exposure room. Aluminum bellows, 1-1/2 inch in diameter, shields the patch cables from the tank to the J box. The signal cables from the J box to the screen room are enclosed in a foil-lined plastic zipper tubing. Cable interconnections are made in the J box, which has an RFI-gasketed door.

Two photographs of the tank setup at HERMES are shown in Figure 2.5. Aluminum disks are used to cover the unused feedthrough ports.

The details of the grounding and shielding are shown in Figure 2.6. One continuous RFI shield, consisting of the tank, bellows, J box, zip tube, patch panel box, and screen room encloses the instrumentation, cabling and sensors. The screen room is doubly shielded with the two shields connected together only at the patch panel. The screen room is connected

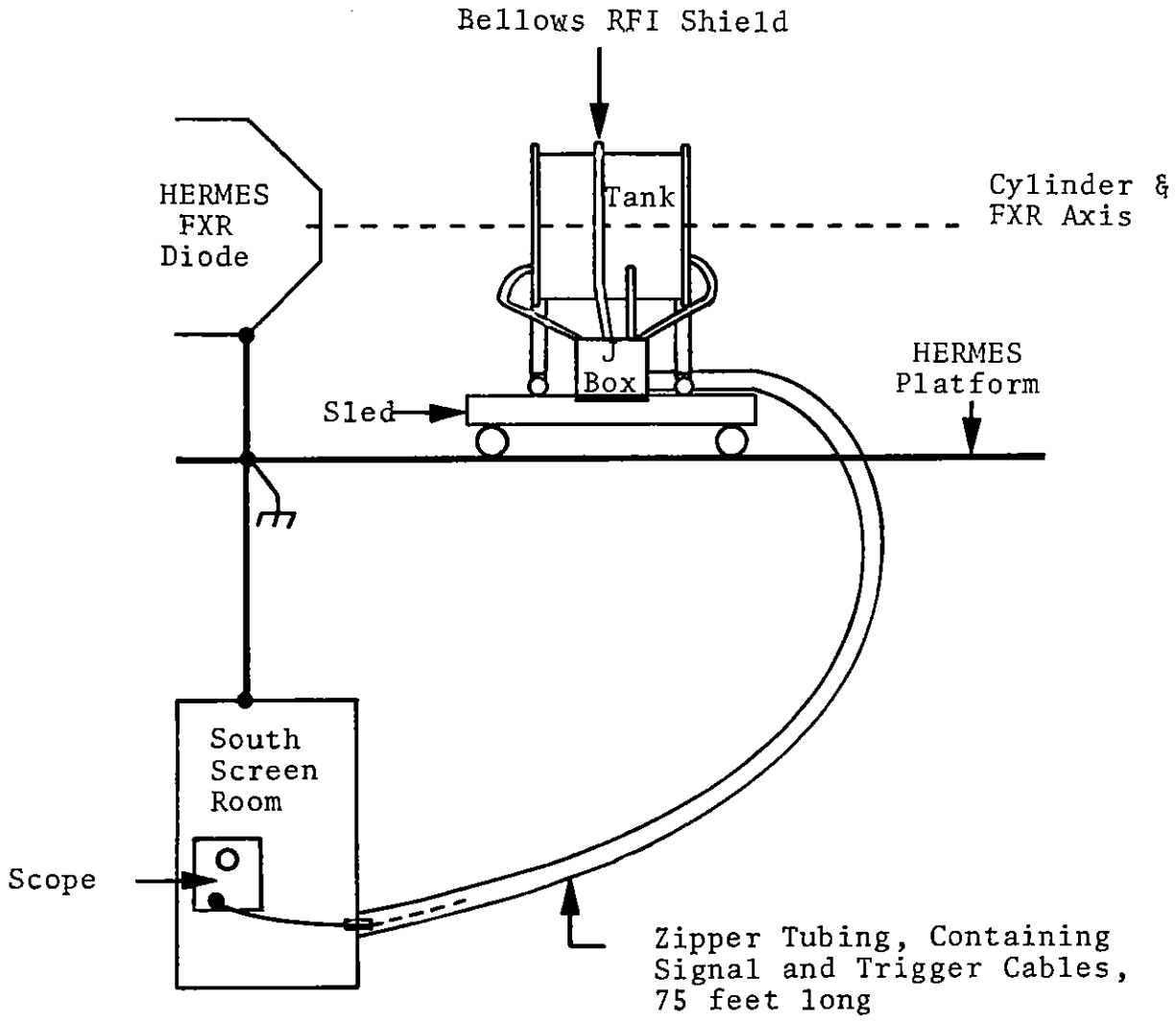

FIGURE 2.4
HERMES Experimental Setup

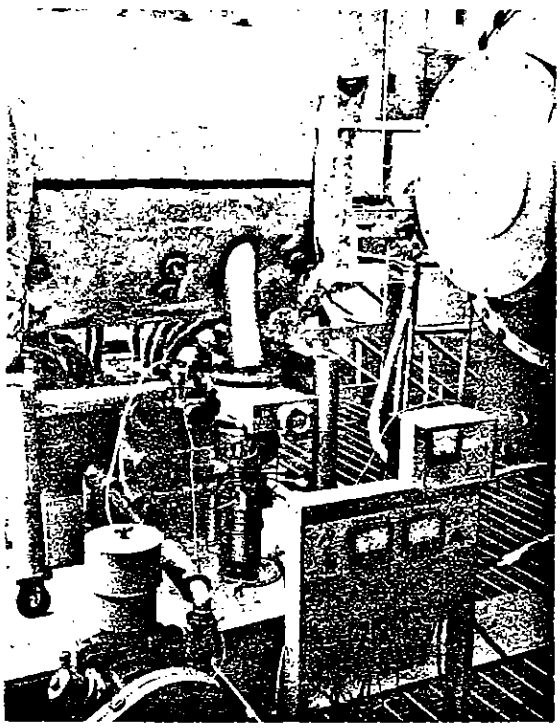

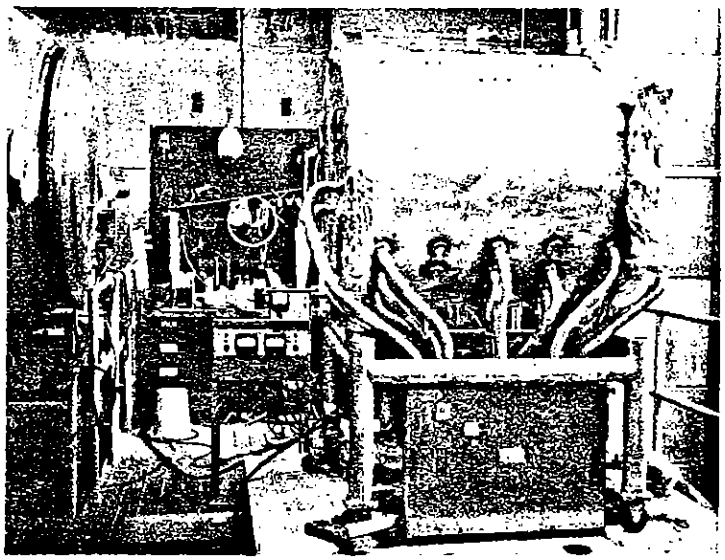

FIGURE 2.5
Photographs of Experimental Setup at HERMES

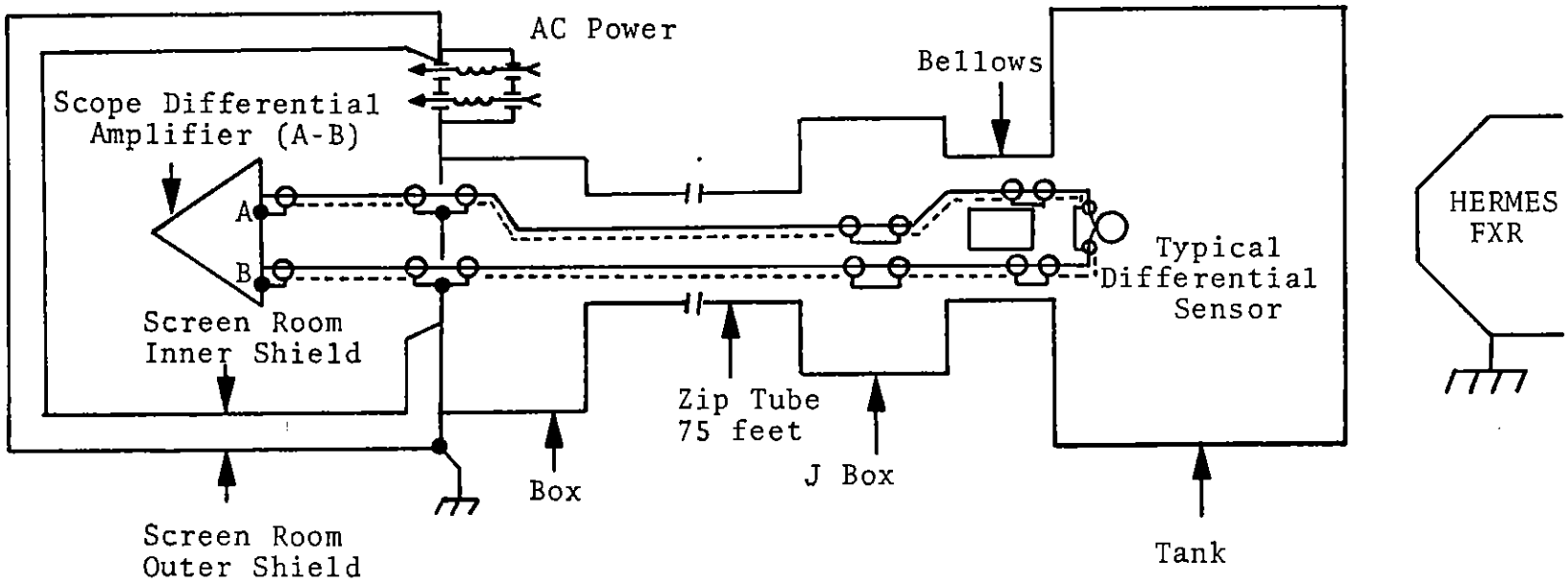

FIGURE 2.6

Shielding and Grounding System at HERMES

to facility ground, as is the FXR machine anode. Instrument power to the screen room is filtered and enters at the patch panel.

Differential connections were used between most sensors and the scopes to cancel noise signals due to electromagnetic coupling, charge transfer and dielectric photoconductivity in the signal leads. The differential signal was separated from the common mode noise at the scope using the A-B provision at the scope vertical amplifier. The cabling for a typical differential sensor is also shown in Figure 2.6. A common ground for all coax shields is necessarily made at the patch panel, due to its design. The coax shields are not directly connected to the tank.

Eighteen coaxial cables, type RG213/U, tied in pairs of equal length, were provided in the zip tube. Two of these cables were set aside for the trigger system, having type N connectors in the J box to mate with the PIN diode. The remaining eight pairs had GR874 connectors compatible with the patch cable ends in the J box for ease in interconnecting. The cable ends at the screen room patch panel and at the tank feedthrough ports required HN connectors. All cabling was 50 ohm characteristic impedance, and was terminated at each end whenever practical. All differential cabling was checked for equal delays by simultaneous pulsing with an SKL503 pulse generator and matched tee.

2.3 INSTRUMENTATION

Data recording was accomplished with high-frequency oscilloscopes to preserve faithfully the rise times and oscillations expected in the waveforms. The project requested and received ten Hewlett-Packard type 183B scopes with cameras from the DNA inventory. Five scopes were obtained with the 100 MHz vertical amplifier and the remaining five with the

250 MHz amplifier. A Tektronix 454 scope with 150 MHz bandwidth was borrowed from Sandia for the tests, since its high impedance inputs were required by the passive integrators used with the Rogowski coil. The signal inputs of the HP183B scopes are internally terminated in 50 ohms.

A manually actuated control system to operate all camera shutter solenoids simultaneously was supplied by S^3. Sweep speeds were ordinarily 20 nsec/cm. Polaroid type 410 high-speed roll film was used to obtain good trace definition.

The trigger system consisted of a PIN diode, power supply, and fanout networks and is shown in Figure 2.7. The PIN diode used was a Model No. 025-PIN-125 Pulsed X-Ray detector manufactured by Solid State Radiations, Inc. The silicon chip is conveniently mounted in a type N coaxial connector. The detector was located in the bottom of the junction box, within an enclosure made of lead bricks to reduce the dose.

A battery-powered bias supply for the detector was built by S^3. It consists of three 67-1/2 volt batteries, a 10 Kohm charging resistor, a 0.1 μf coupling capacitor, and an on-off switch. The RC time constant of the supply operating into a 50 ohm load is 5 μsec, long compared to the HERMES pulse. The capacitor output is therefore a good representation of the diode photocurrent and was monitored on each shot for dosimetry.

The trigger output is connected to two fanout networks in series. The input to the second network is delayed approximately 70 nsec to compensate for the signal delay line within each 100 MHz plug in.

The vacuum monitor system consisted of a discharge gauge, thermocouple gauges, and thermistor gauges, with their controllers. The three types are summarized in Table 2.2. The Veeco system and one Bendix system monitored the diffusion and fore pump pressures outside the shield. A second Bendix

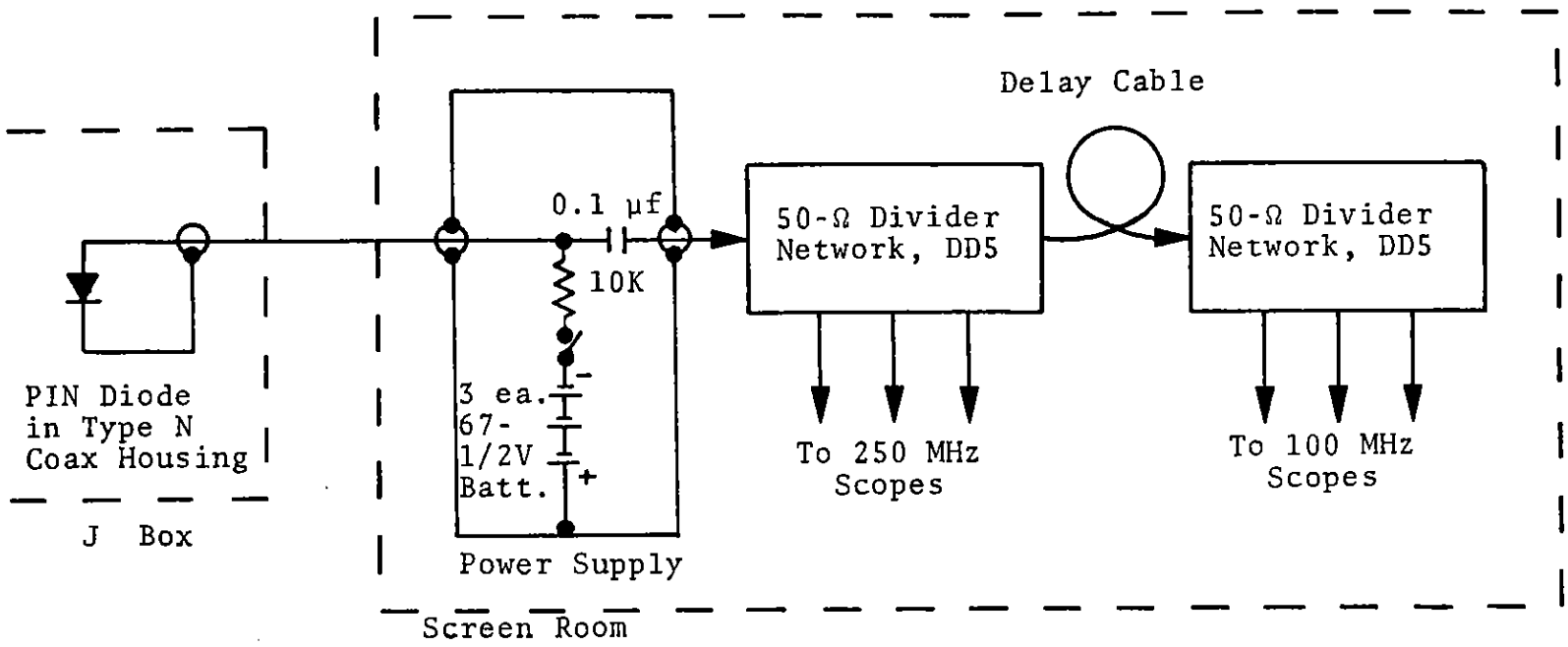

FIGURE 2.7
PIN Trigger System

system monitored the tank vacuum directly, entirely within the RFI shield. The thermistor gauge was inserted into a feedthrough port and the controller placed in the screen room so that vacuum at shot time was easily recorded. All gauges were electrically isolated from the tank.

TABLE 2.2
VACUUM GAUGES AND CONTROLLERS

Type	Gauge Model No.	Controller Model No.	Useful Pressure Ranges*
Discharge Tube	Veeco DG-2-11	DG2-2T	$<10^{-1}$ μ - 10 μ
Thermocouple	Veeco DV-1M		10 μ - 1 Torr
Thermistor	Bendix GT-034	GT-340	1 μ - 760 Torr

*Not necessarily the full range specified by the manufacturer.

The vacuum obtainable with the fore pump alone was approximately 1 Torr. The ultimate vacuum reached with the diffusion pump was approximately 0.3 microns. Intermediate values were set with an adjustable leak valve, a needle valve fitted with a micrometer dial.

3. SENSORS

3.1 INTRODUCTION

The five sensor types used for IEMP measurements on this project are listed in Table 3.1. This section discusses the theory, construction and calibration of these sensors.

TABLE 3.1
IEMP SENSORS

Sensor	Measured Quantity
Moebius Loop	Magnetic Field
Parallel Grid Dipole	Electric Field
Wall Current Assembly	Return Current in Wall
Rogowski Coil	Electron Current Density
Current Probes	Cable Sheath Currents

Many of the sensors were provided with balanced signal distribution, consisting of a pair of coaxial cables connecting the sensor to the oscilloscope. This scheme was used to cancel the extraneous signals induced in each cable due to incident photons and electrons. The A-B feature of the scope vertical amplifier was used to reconstitute the differential signal from the common mode noise.

3.2 MAGNETIC FIELD SENSORS

The magnetic field sensors used by this project are low-impedance Moebius strip loops encapsulated in epoxy, similar to those conceived by C. Baum, AFWL.[2] The loops respond to the time derivative of the magnetic field component normal to

the loop plane. Their time constants are much smaller than the frequency component periods of interest at HERMES. The loop operation is based on Faraday's law, which reduces here to

$$V = \dot{B} A n$$

where V is the loop output voltage in volts, $\dot{B}$ is the derivative of the average magnetic flux density normal to and enclosed by the loop in Teslas (webers/m^2), A is the loop area in square meters, and n is the number of loop turns.

The loops have twice the output of a conventional split shield loop and have much less sensitivity to radiation-induced noise, due to the symmetry inherent in the design. They are potted in epoxy to minimize the effects of conducting plasma in the vicinity. Three sensor types were used and their characteristics are presented in Table 3.2. The actual loops were fabricated at S^3 and used on a previous IEMP program. This project modified the output connections of two types of balanced loops, to improve the signal-to-noise ratio and the impedance matching.

TABLE 3.2
MAGNETIC FIELD ($\dot{B}$) SENSORS

Type	Area	No. Turns	Output	Sensitivity volts/gauss/nsec
Miniature (toroidal)	2 cm^2	2	Differential	40
Small (cylindrical)	20 cm^2	2	Differential	400
Small (cylindrical)	20 cm^2	1	Single Ended	200

The construction of the differential toroidal loop is illustrated in Figure 3.1. The sensor is aluminum micro-coax cable, Type UT93, manufactured by Uniform Tube, Inc.,

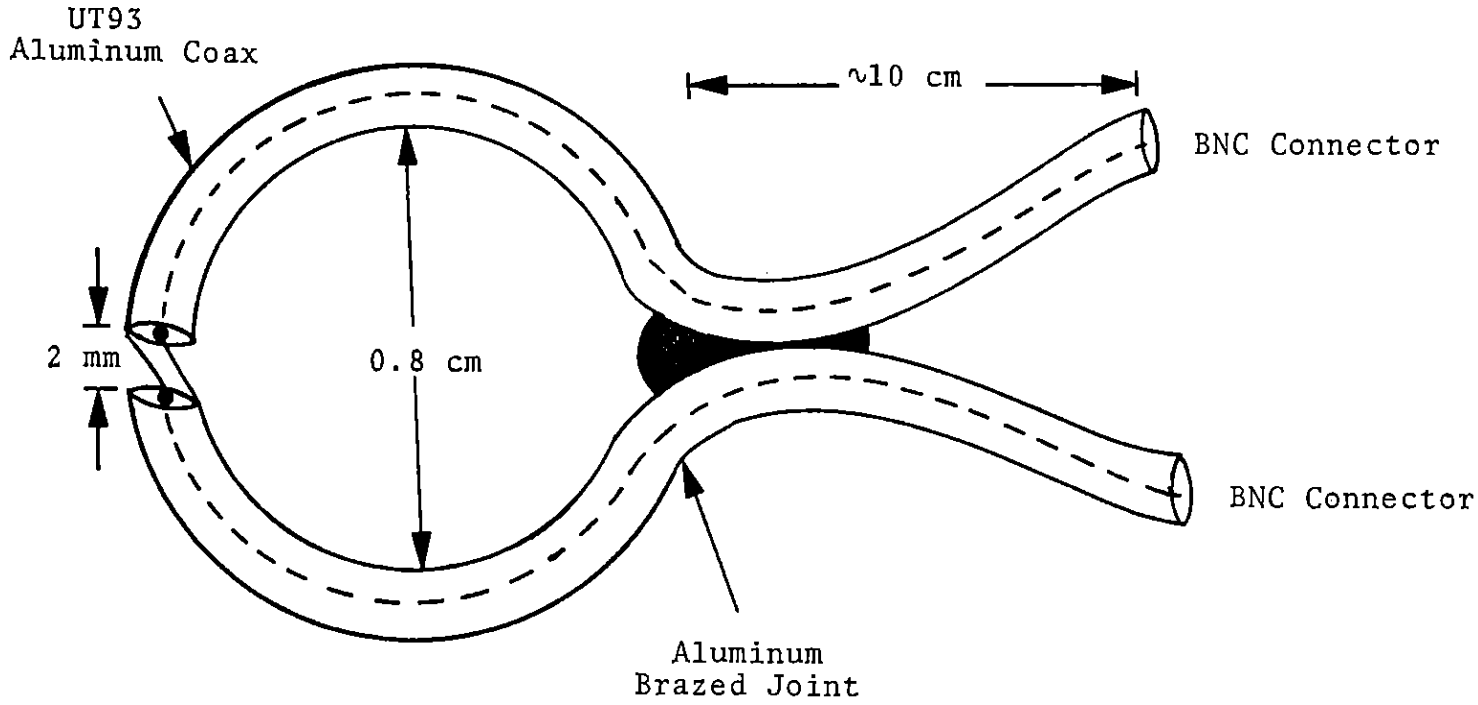

FIGURE 3.1
Differential Toroidal Loop

which was brazed with aluminum alloy to form a loop. The Faraday voltage appears across the 2 mm gap at the top of the loop. The Moebius connection is made at the gap between each center conductor and the appropriate outer conductor and produces a two turn symmetrical loop. The loop area is 2 cm^2, yielding a sensitivity of 40 volts per gauss/nsec. The coax tubes were terminated in BNC connectors. The loop itself was potted in Shell Epon 828 epoxy. A photograph of one of these miniature sensors is shown in Figure 3.2.

The small differential cylindrical loop is constructed as shown in Figure 3.3. The electrical circuit is essentially the same as in the miniature loop. The cylinder, formed of performated aluminum sheet, 0.020 inch thick, and the second micro-coax loop both serve to lower the loop inductance and maintain the impedance match to the gap. The output is a

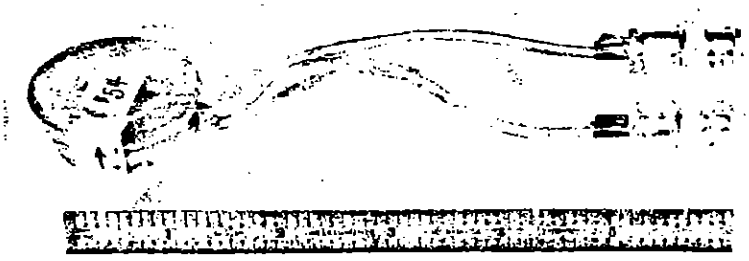

FIGURE 3.2
Photograph of Miniature $\dot{B}$ Sensor

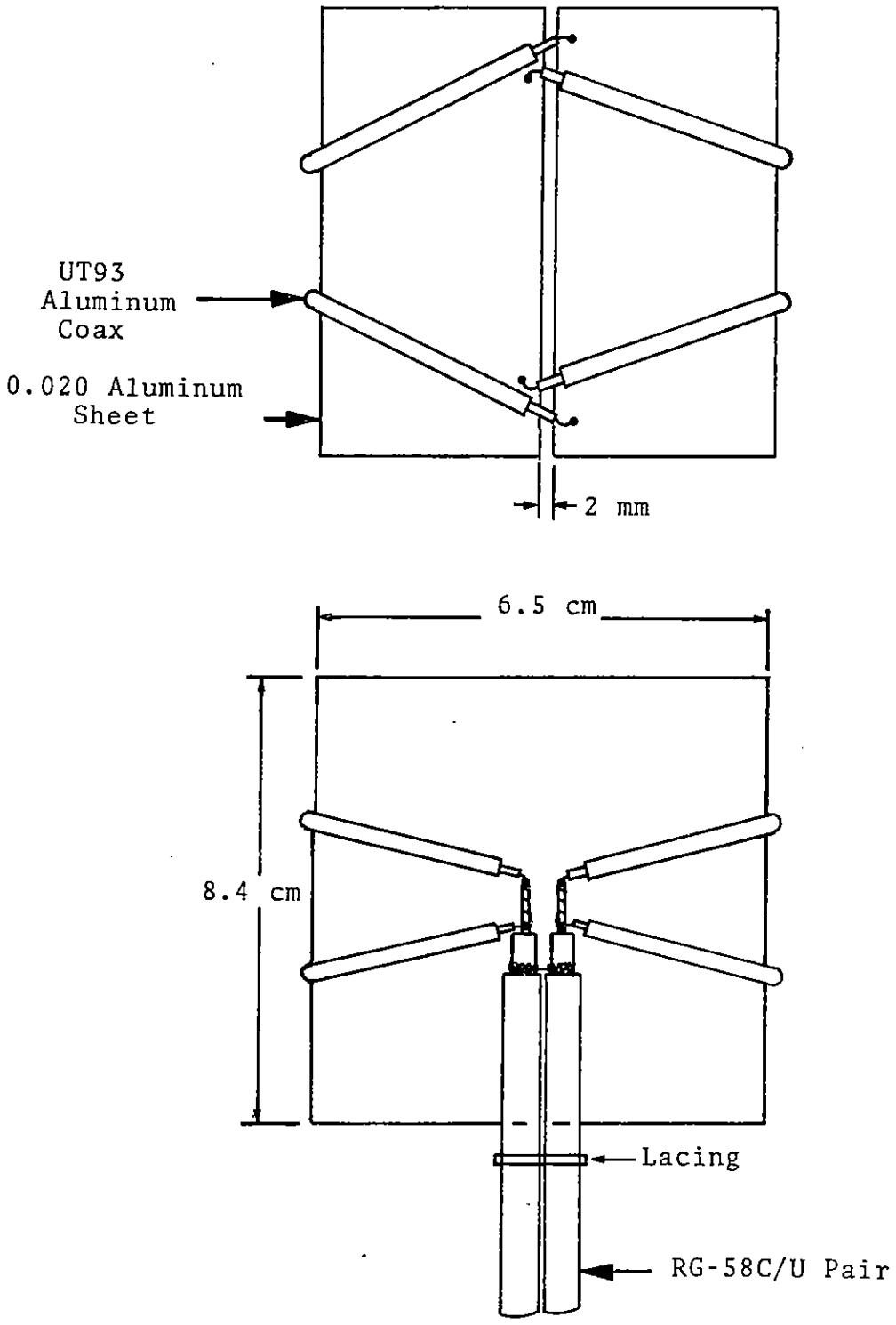

FIGURE 3.3
Differential Cylindrical Loop